Available online at www.sciencedirect.com
SCIENCE DIRECT
Biochemical Pharmacology 70 (2005) 1298–1308
Biochemical Pharmacology
www.elsevier.com/locate/biochempharm

A novel LXR-α activator identified from the natural product *Gynostemma pentaphyllum*

Tom Hsun-Wei Huang [1], Valentina Razmovski-Naumovski [1], Noeris K. Salam, Rujee K. Duke, Van Hoan Tran, Colin C. Duke, Basil D. Roufogalis *

Pharmaceutical Chemistry, Herbal Medicines Research and Education Centre, Faculty of Pharmacy, A15, S322, University of Sydney, NSW 2006, Australia

Received 6 June 2005; accepted 28 July 2005

Abstract

Liver X receptors (LXR) play an important role in cholesterol homeostasis by serving as regulatory sensors of cholesterol levels in tissues. The present study reports a novel LXR-α activator, (20*S*)-2α, 3β, 12β, 24(*S*)-pentahydroxydammar-25-ene 20-*O*-β-D-glucopyranoside (TR1), a dammarane-type gynosaponin, isolated from the herbal medicine, *Gynostemma pentaphyllum*. Gynosaponin TR1 demonstrated greater selectivity toward activation of the LXR-α isoform than LXR-β in HEK293 cells. TR1 selectively enhanced LXR-mediated transcriptional activation and protein expression of ABCA1 and apoE gene expression and secretion in THP-1-derived macrophages. The selectivity of TR1 for LXR-α was consistent with ligand docking studies, which showed favourable interaction of TR1 in the LXR-α-binding domain, whereas the presence of the sugar substituent interfered with binding to the LXR-β site. Findings from the present study may provide insight into the development of pharmaceutical agents for treating atherosclerosis.

Keywords: Liver X receptor; ABCA1; Apolipoprotein E; Gynosaponin; Gypenoside; *Gynostemma pentaphyllum*

1. Introduction

A global research effort has led to significant advances in therapeutic treatments toward preventing or curing cardiovascular disease (CVD). Vascular biology has revealed much information on the pathophysiology of atherosclerosis [1,2], from the first report of its association with cholesterol [3], to the current notion that inflammation and the immune response also contribute to atherogenesis [1,4]. An important target for pharmacological intervention is through the up-regulation of reverse cholesterol transport (RCT), whereby cholesterol is removed from macrophages and other peripheral cells and transported to the liver by plasma lipoproteins for excretion as bile salts [5]. These systemic changes involve regulation of the expression of a myriad of genes through ligand-activated transcription factors called nuclear receptors. One particular therapeutic target, known as transcription factor liver X receptor (LXR), regulates RCT by functioning as a sensor of cholesterol levels in tissues [6–8].

At present, two LXR isoforms have been characterised. LXR-α (NR1H3) is primarily expressed in the liver, intestine, adipose tissue, spleen and macrophages, whilst LXR-β (NR1H2) is ubiquitously expressed [6]. LXR-α and LXR-β share considerable sequence homology (~77% identity in DNA- and ligand-binding domains) and appear to respond to the same endogenous ligands [9]. Both receptors are activated by naturally occurring oxysterols, such as 22(*R*)- and 24(*S*)-hydroxycholesterol [10] and 24(*S*)- and 25-epoxycholesterol [9] and by synthetic agonists, such as T0901317 [11,12], GW3965 [13] and acetylpodocarpic dimmer [14].

Theoretical investigations of the known LXR agonists have provided much insight in the understanding of the LXR ligand-binding domain (LBD) [15,16] and identification of the the specificity towards each LXR isoform [17,18]. The recent reported X-ray crystal structures of

Abbreviations: ABC, ATP-binding cassette; apoE, apolipoprotein E; CVD, cardiovascular disease; glu, glucose; HDL, high-density lipoprotein; LXR, liver X receptor; RCT, reverse cholesterol transport; RT, room temperature; VLDL, very-low-density lipoprotein

* Corresponding author. Tel.: +61 2 9351 2831; fax: +61 2 9351 4447.
E-mail address: basilr@pharm.usyd.edu.au (B.D. Roufogalis).
[1] These authors contributed equally.

0006-2952/$ – see front matter © 2005 Elsevier Inc. All rights reserved.
doi:10.1016/j.bcp.2005.07.033

human LXR-α and LXR-β LBDs complexed with 24(*S*), 25-epoxycholesterol, T0901317 and GW3965 provide insight into key elements of ligand recognition as well as the mechanisms of activation for each ligand [12]. The LBDs share a common, mainly α-helical fold that embeds a hydrophobic ligand-binding pocket. The structures have shown that ligands can affect the conformation of the ligand-dependent activation function 2 residing in the C-terminal H12. Therefore, an agonist allows H12 to cover the ligand-binding pocket, thereby providing one of the sides in the coactivator-binding pocket [19]. Furthermore, this ligand-activation of the LXR transcription factors results in the formation of obligate heterodimers with the retinoid X receptor. The complexes subsequently bind to the consensus response element sequence DR4 in the promoter regions of several target genes, including cholesterol 7α-hydroxylase, cholesterol ester-transfer protein, ATP-binding cassette (ABC) transporter proteins (ABCA1, ABCG5 and ABCG8), apolipoprotein E (apoE), lipoprotein lipase and sterol-response element-binding protein-1c [8,20].

The ABCA1 protein is critical for the first step in the RCT pathway through its up-regulation in lipid-loaded macrophages and its involvement in the efflux of excess cellular cholesterol to apolipoprotein acceptors. Humans who are genetically deficient in ABCA1 due to mutations in both ABCA1 alleles (homozygous Tangier disease) lack high-density lipoprotein (HDL) cholesterol almost completely, resulting in the accumulation of cholesterol esters in peripheral macrophages, leading to a greater risk of atherosclerosis [21,22]. Numerous studies have shown ABCA1 to be a definite LXR target gene both in vitro and in vivo. The increase in cholesterol efflux by LXR ligands was shown to be ABCA1-dependent, as the effect of ligands was lost in the ABCA1-deficient Tangier fibroblasts. The ability of LXRs to control ABCA1 expression appears to be a significant factor in the enhanced HDL levels in mice [23].

ApoE is another essential LXR target gene in cholesterol metabolism. ApoE mediates the hepatic uptake of very-low-density lipoprotein (VLDL) and chylomicron remnants and can serve as an extracellular acceptor for cholesterol in the ABCA1 efflux pathway [24]. In contrast to ABCA1, regulation of apoE by LXR is tissue-specific, occurring only in macrophages and adipocytes [13]. The beneficial nature of apoE production by macrophages is evident from several animal studies. Mice expressing apoE only in macrophages were protected against atherosclerosis, whereas those specifically lacking apoE expression in macrophages were more susceptible [9,25,26]. Therefore, induction of the ABCA1 and apoE gene by LXR agonists might lead to a decreased cholesterol burden in the arterial wall, as well as enhanced HDL levels [5,27].

Identifying potential medicinal compounds from nature with increasing efficacy and safety has become important in the growing population of pre-dyslipidaemic patients, as well as patients suffering from related CVD events [28]. Recently, the first non-oxysterol natural product ligand of LXR from *Penicillium paxilli* was discovered. The indole alkaloid fungal metabolite, paxilline, functions as a ligand for both LXR-α and LXR-β. Unfortunately, the clinical application of paxilline is limited by its tremorgenic mycotoxin properties and antagonism of high conductance calcium-activated K channels [29]. To date, there has been no report of LXR agonists from plant-derived material.

Gynostemma pentaphyllum (Cucurbitaceae), known as *Jiagulan* in Chinese herbal medicine, is a perennial vine endemic to southern China, Japan, India and Korea [30]. The pharmacological studies of *G. pentaphyllum* have illustrated a variety of biological activities, including anti-inflammatory, anti-tumour, immunopotentiating, anti-ulcer, anti-oxidant and retardation of aging [30–32]. *G. pentaphyllum* has been used clinically in China and has been described as having minimal toxicity [33,34]. The dammarane saponins, namely gypenosides or gynosaponins, isolated from *G. pentaphyllum* are believed to be the active principles responsible for its biological activities and reported clinical effect of the *G. pentaphyllum* extract in the treatment of CVDs and related disorders [31,35]. However, the mode of action of gypenosides has not been well-defined. Due to their similarity in structure to the oxysterols (Fig. 1), we postulated that *G. pentaphyllum* may contain novel LXR agonist(s) with similar biological and ligand-binding properties.

In the present study, we demonstrate that the new dammarane saponin, gynosaponin TR1 ((20*S*)-2α, 3β,

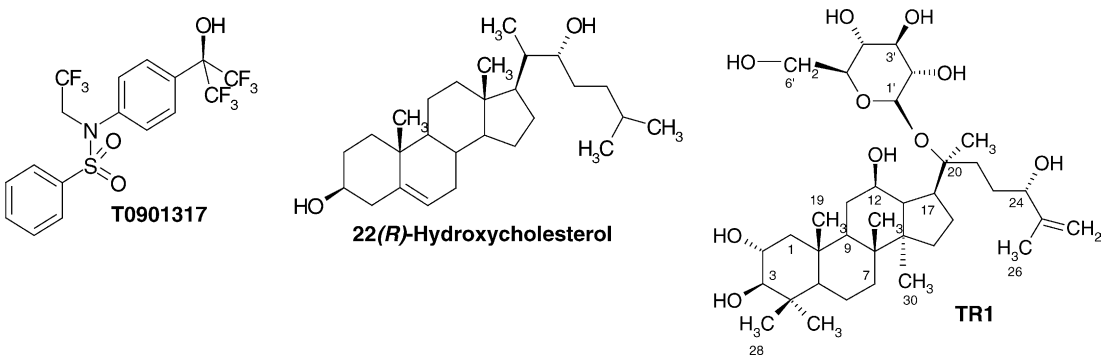

Fig. 1. Structure of T0901317, 22(*R*)-HC and TR1.

12β, 24(*S*)-pentahydroxydammar-25-ene 20-O-β-D-glucopyranoside), isolated from *G. pentaphyllum*, is an agonist of LXR, with selectivity for LXR-α over LXR-β. Furthermore, it was also found to be an inducer of ABCA1 and apoE gene expression in vitro. Theoretical investigations were also employed to rationalise the selectivity of TR1 to LXR-α through an understanding of its potential binding interactions.

2. Materials and methods

2.1. Chemicals and reagents

Anti-actin rabbit primary antibody, anti-goat-IgG peroxidase-conjugated secondary antibody, β-mercaptoethanol, 22(*R*)-hydroxycholesterol (22(*R*)-HC), Tween 20, *O*-phenylenediamine dihydrochloride and phorbol 12-myristate 13-acetate (PMA), deuterated (d_5)-pyridine (C_5D_5N) 99.5 at.% and filter agent Celite 521 were obtained from Sigma (Australia). T0901317 was purchased from Cayman chemical (USA). Silica gel 60H and 60H silanised (normal and reversed phase, respectively) were purchased from Merck Pty. Ltd. (Australia). Dichloromethane, ethanol, methanol and HPLC-grade acetonitrile were purchased from Asia Pacific Specialty Chemicals Ltd. (APS, Australia). Analytical grade solvents were distilled prior to use. A C-18, 5 μm, 21.2 mm × 50 mm Luna preparative HPLC column was purchased from Phenomenex (Australia). ^{13}C and ^{1}H NMR, DEPT, COSY and HETCOR spectra were obtained on a Varian Gemini 300 MHz Instrument (USA). Initial mass data were measured on a ThermoFinnigan TSQ 7000 liquid chromatography–mass spectrometer (LC–MS/MS) (San Jose, USA). Positive high-resolution mass spectrometry (HRESI–MS) was carried out on a Bruker BioApex-II 7T FTICR mass spectrometer equipped with both an on- and off-axis Analytica ESI source. Data acquisition (typically 512 K spectra) and processing were performed using XMASS™ (Version 6.2 Software, Bruker Daltonics, USA).

2.2. Extraction, isolation and identification of TR1 from G. pentaphyllum

Dried locally grown *G. pentaphyllum* plant material (1184 g) was extracted three times with 10% methanol in water with stirring at room temperature (RT). The residue was subsequently extracted three times with ethanol at RT. The ethanol extract (GPE; 40 g) was dissolved in dichloromethane:ethanol (5:1) (with a few drops of water and methanol to aid the dissolution) and loaded onto a normal-phase silica gel short-column vacuum chromatography column (NPSC). A step-wise gradient of eluents consisting of dichloromethane:ethanol (5:1, 4:1, 3:1, 2:1, 1:1, 1:2, 0:1) was employed to obtain various eluate fractions (100 mL). The column was finally eluted with 100% methanol (200 mL) followed by 20% methanol in water (200 mL). The fractions were concentrated to dryness under reduced pressure using a rotary evaporator and analysed by thin-layer chromatography (TLC). Fractions with similar TLC profiles were combined and further purified using NPSC, as described above. A similar purification procedure was repeated twice to isolate potential candidates. Finally, reversed-phase silica gel short-column vacuum chromatography (RPSC) and HPLC were employed to further purify individual saponins. A step-wise gradient of eluents for RPSC consisting of methanol:-water (20:80, 30:70, 40:60, 50:50, 60:40, 70:30, 80:20) followed by 100% methanol to elute the sample (2.75 g) and the fractions (100 mL) were collected and concentrated to dryness under reduced pressure. The saponin (512 mg) collected at 60:40 (methanol:water) was subjected to preparative HPLC using an isocratic condition of 32.5% acetonitrile in water and detected at 210 nm to give the gynosaponin TR1 as colourless plate-like crystals. NMR and mass spectra of TR1 were analysed using instruments as described above.

2.3. Tissue culture

The THP-1 human monocytic cell line was a kind gift from Dr. Asne Bauskin (St. Vincent's Hospital, Australia). The human embryonic kidney 293 cell line (HEK293) was obtained from the American-Type Culture Collection (USA). All materials used for tissue culture were purchased from Invitrogen, Australia unless specified. HEK293 was grown in DMEM/F12, containing L-glutamine supplemented with penicillin (100 U/mL), streptomycin (100 μg/mL) and 10% (v/v) heat-inactivated foetal bovine serum in a humidified atmosphere of 5% CO_2 and 95% O_2 at 37 °C. THP-1 monocytes were maintained in RPMI 1640 containing the supplementary ingredients as mentioned above, with the addition of 55 μM β-mercaptoethanol. Differentiated THP-1 macrophages were obtained by inducing the monocyte with 50 ng/mL PMA for 3 days [37,38]. Cytotoxicity of the ligands (T0901317, 22(*R*)-HC and TR1) on the cells was assessed using cell viability assays. All compounds showed little or no effect on cell viability (>90% viability remained) at the concentrations examined (data not shown).

2.4. Transfection and luciferase assay

The transfection and luciferase procedures were performed using HEK293 cell lines as described previously [11,29,39]. The plasmids used for transfection were hLXREx3TK-Luc plasmid (a kind gift from Dr. Barry M. Forman, City of Hope National Medical Center, USA), pCMX-hLXR-α and pCMV-hLXR-β plasmids (a kind gift from Dr. Alan Tall, Columbia University, USA). The pSV-β-galactosidase control vector (Promega, Australia) was used to normalise the transfection efficiencies.

Cells were transfected with FuGENE 6 transfection reagent (Roche Applied Science, USA) in accordance with the manufacturer's instruction. After 24 h, the cells were harvested and plated on growth media in 96-well plates at 5×10^4 cells/well and allowed to attach for 2 h. The cells were then treated with LXR ligands (T0901317 and 22(*R*)-HC) and TR1 or vehicle (0.1% DMSO) for 24 h. After 24 h, the cells were lysed and assayed for luciferase and β-galactosidase activities using the Bright-Glo Luciferase Assay System and Beta-Glo Assay System (Promega, Australia), respectively. The results were expressed as relative luciferase activity (fold difference compared to negative control).

2.5. Semi-quantitative mRNA analysis

Total RNA was extracted from THP-1-derived macrophages using TRIzol reagent (Invitrogen, Australia) after 2 days (for LXR-α and ABCA1 in THP-1 macrophage), 3 days (for apoE in THP-1 macrophage) treatment with LXR ligands (T0901317 and 22(*R*)-HC) and TR1 or vehicle (0.1% DMSO). The relative levels of specific mRNAs were assessed by reverse transcription polymerase chain reaction (RT-PCR) following the method reported in the literature [40]. The sequences of the sense and antisense primers used for amplification were: LXR-α (HSU22662: 332bp), 5′-CGGGCTTCCACTACAATGTT-3′ and 5′-CTTCTCGATCATGCCCAGTT-3′; ABCA1 (NM005502: 462bp), 5′-AAGCACTTCCTCCGAGTCAA-3′ and 5′-TGACAGGCTTCACTCCACTG-3′; apoE (NM000041: 443bp), 5′-AGAAGCGCCTGGCAGTGTA-3′and 5′-CTTCGGCGTTCAGTGATTGT-3′; β-actin (NM001101: 629bp), 5′-GGAGTAACCAGGTCGTCCAA-3′ and 5′-GAAGGTGCCCAGAATACCAA-3′. The quantity and base pair size of the PCR generated DNA fragments were estimated relative to DNA ladder standards. RT-PCR values are presented as a ratio of the specified gene signal in the selected linear amplification cycle divided by the β-actin signal.

2.6. Protein extraction and semi-quantitative immunoblotting

Immunoblotting was conducted as previously described [41,42]. The cells (THP-1 monocyte and derived macrophage) were treated with LXR ligands (T0901317 and 22(*R*)-HC) and TR1 or vehicle (0.1% DMSO) for 2 days. The cell were lysed and centrifuged at 16,000 × *g* (SS-34 rotor, Sorvall Centrifuge, USA) for 30 min and supernatants resolved by reducing SDS-PAGE (6–10% polyacrylamide gels). Protein was transferred on to PVDF membranes with Dunn–carbonate transfer buffer [10 mM sodium bicarbonate, 3 mM sodium carbonate and 15% MeOH at 4 °C] and blocked in 5% skim-milk powder overnight. The membrane was then incubated with anti-human LXR-α polyclonal primary goat antibody (1:700 dilution; Santa Cruz Biotechnology, USA) or anti-human ABCA1 polyclonal primary rabbit antibody (1:600 dilution; Novus Biologicals, USA). After membrane washing, horseradish peroxidase conjugated anti-goat (1:5000 dilution) or anti-rabbit (1:5000 dilution) secondary antibodies were applied (Promega, Australia). Bound antibodies were detected using enhanced chemiluminescence with Lumi-Light Western Blotting Substrate (Roche, Australia). To quantify the protein expression of LXR-α and ABCA1, the intensity of the signal on the membrane was normalised to actin. The membranes were re-probed with anti-actin primary antibody (1:1000 dilution) after stripping with boiling distilled water for 5 min. The membranes were then washed and re-incubated with the horseradish peroxidase conjugated anti-rabbit secondary antibody as described above. Protein content was determined by the Bradford assay method using bovine serum albumin as a standard [43].

2.7. ApoE quantification

ApoE in culture medium was measured by enzyme-linked immunosorbent assays (ELISA), as described previously [37]. Briefly, THP-1-derived macrophages were incubated for 3 days with 0.77 ng/mL of PMA in the presence of the LXR ligands (T0901317 and 22(*R*)-HC) and TR1 or vehicle (0.1% DMSO). Cell supernatants were collected and diluted (five-fold) with ELISA buffer, then 100 μL aliquot was added to each well of the ELISA plate. After 1 h incubation at 37 °C, the plate was washed three times with washing buffer (200 μL) [PBS with 0.1% Tween 20], then incubated with anti-human apoE IgG goat primary antibody (1:10,000 dilution; 100 μL/well Calbiochem, USA) for 1 h at 37 °C on an orbital Mixer Incubator (Rateck Instruments, Australia) at 200 rpm. The plates were subsequently washed three times with washing buffer then incubated with anti-goat-IgG peroxidase-conjugated secondary antibody (1:5000 dilution; 100 μL/well). The plate was then washed five times and incubated with *O*-phenylenediamine dihydrochloride (100 μL/well) solution for 15–20 min with shaking at RT. The reaction was stopped by the addition of sulfuric acid (3 mol/L; 50 μL/well) (Fluka, Australia) and continuous shaking for 1 min at RT. The absorbance was read at 492 nm versus 620 nm with a microplate photometer (POLARstar OPTIMA; BMG Labtech, Australia). Dilutions of known concentrations of human apoE (Chemicon, USA) were used for quantification.

2.8. Statistical analysis

All results are expressed as means ± S.E.M. Data were analysed by one-factor analysis of variance (ANOVA). If a statistically significant effect was found, the Newman–Keuls test was performed to isolate the difference between the groups; *p*-values less than 0.05 ($p < 0.05$) were considered as indicative of significance.

2.9. Ligand docking

The crystal structure of the LXR-α:RXR-β complex bound with T0901317 (PDB 1UHL) was used as the primary model for LXR-α [15]. Similarly, the LXR-β crystal structure bound with the neutral oxysterol 24(*S*), 25-epoxycholesterol was also used (PDB 1P8D) [16]. The structures of TR1 and LXR agonists (T0901317 and 22(*R*)-HC) were initially built using the program Maestro v7.0 (Portland, USA). Each ligand was energy minimised with the MM3* force field prior to docking in MacroModel v8.1 [44]. Docking was performed with each ligand using the Glide software [45]. Here, the best-docked pose was scored and chosen and scored from the calculated binding affinity; the receptor–ligand molecular mechanics interaction energy and ligand strain energy. Furthermore, the poses were subjected to another final optimisation procedure in which the receptor–ligand complex underwent a full molecular mechanics energy minimisation (OPLS–AA force field) in order to optimise flexible side-chain residues of LXR that may interact with the ligands. The minimised complex was retained as the final model and was applied in subsequent investigations.

3. Results

3.1. Identification of (20S)-2α, 3β, 12β, 24(S)-pentahydroxydammar-25-ene 20-O-β-D-glucopyranoside (TR1)

The title compound was identified as (20*S*)-2α, 3β, 12β, 24(*S*)-pentahydroxydammar-25-ene 20-*O*-β-D-glucopyranoside, as shown in Fig. 1. The amount of TR1 recovered was 57 mg. Electrospray liquid chromatography–mass spectrometry (ESI–MS) analysis gave a molecular ion of *m/z* 672.5 $[M + NH_4^+]^+$ and a fragment ion at *m/z* 475.2 $[(M - glu) + 1]^+$. Positive high-resolution mass spectrometry (HRESI-MS) analysis showed a molecular ion at *m/z* 677.421909 (observed for $C_{36}H_{62}O_{10}Na$); 677.42355 (calculated for $C_{36}H_{62}O_{10}Na$), thus, the molecular formula of TR1 was tentatively established as $C_{36}H_{62}O_{10}$.

^1H and ^{13}C nuclear magnetic resonance (NMR) of TR1 were compared to that of gynosaponin TN1 [46], gypenoside LXXI and ginsenoside M_{7cd} LXXI and ginsenoside M_{7cd} [36]. ^{13}C nuclear magnetic resonance spectrum data of the compound is shown below:

^{13}C NMR (75 MHz, in pyridine-d_5) δ;
Aglycone (CH): 68.7 [C2], 83.7 [C3], 56.5 [C5], 50.3 [C9], 70.2 [C12], 49.4 [C13], 51.9 [C17], 75.6 [C24]; (CH_2): 48.4 [C1], 18.8 [C6], 35.1 [C7], 30.6 [C11], 30.8 [C15], 26.7 [C16], 32.5 [C22], 31.2 [C23], 109.9 [C26]; (CH_3): 15.9 [C18], 17.3 [C19], 22.7 [C21], 18.6 [C27], 29.2 [C28], 17.4 [C29], 17.6 [C30];
C: 39.9 [C4], 40.1 [C8], 38.5 [C10], 51.5 [C14], 83.5 [C20], 149.8 [C25];
Glucose (CH): 98.3 [C′1], 75.2 [C′2], 79.1 [C′3], 71.7 [C′4], 78.3 [C′5]; (CH_2): 63.1 [C′6].

3.2. Effect of TR1 and other LXR ligands on LXR-α and-β luciferase activity in HEK293 cell line

Due to the structural similarity of oxysterol 22(*R*)-HC and gynosaponin TR1, their relative potencies and efficacy on LXR-α and LXR-β were compared over similar dose ranges (Fig. 2) [10]. T0901317 (0.01, 0.1 and 1 μM), a well-known agonist of LXR-α and LXR-β, induced dose-dependent increases in LXR-α (1.4-, 2.1- and 4.1-fold) and LXR-β (1.5-, 1.9- and 2.9-fold) activities, respectively (Fig. 2), consistent with previous results [11,12]. Differences in selectivity of activation of the two LXR isoforms were found between 22(*R*)-HC and TR1 over the same concentration range (0.1, 1 and 10 μM). 22(*R*)-HC showed significant activation of both isoforms at 1 and 10 μM, whilst at 10 μM, TR1 showed significant elevation of luciferase activity for LXR-α only (Fig. 2). This selectivity for TR1 on LXR-α is probably due to the presence of the carbohydrate group, which is absent in 22(*R*)-HC. The oxysterol stereoisomer 24(*S*)-HC also activated both LXR-α and LXR-β isomers (results not shown).

3.3. TR1 induces LXR-α and ABCA1 mRNA and protein expression in THP-1-derived macrophages

The induction of ABCA1 gene by agonist activation of LXR expression in macrophages is well-characterised

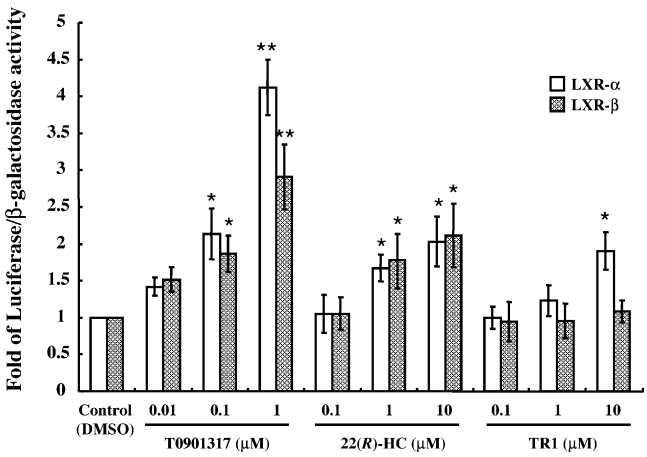

Fig. 2. TR1 selectivity towards LXR-α over LXR-β transactivation compared to known oxysterols in HEK293 cell line. The HEK293 cells were transiently transfected with hLXREx3TK-Luc as a reporter plasmid, pCMX-hLXR-α or pCMV-hLXR-β as expression vectors and pSV-β-galactosidase as a reference plasmid. Cells were treated with increasing concentrations of 22(*R*)-HC (0.1, 1 and 10 μM) and TR1 (0.1, 1, 10 μM). T0901317 (0.01, 0.1 and 1 μM) was used as positive control and DMSO (0.1%) as negative control. At the end of the incubation period, the cells were lysed and assayed for luciferase and β-galactosidase activities were determined. The results are expressed as relative luciferase activity (fold difference compared to negative control). All values are means ± S.E.M. ($n = 3$, each in duplicate) vs. control, $^*p < 0.05$ and $^{**}p < 0.01$.

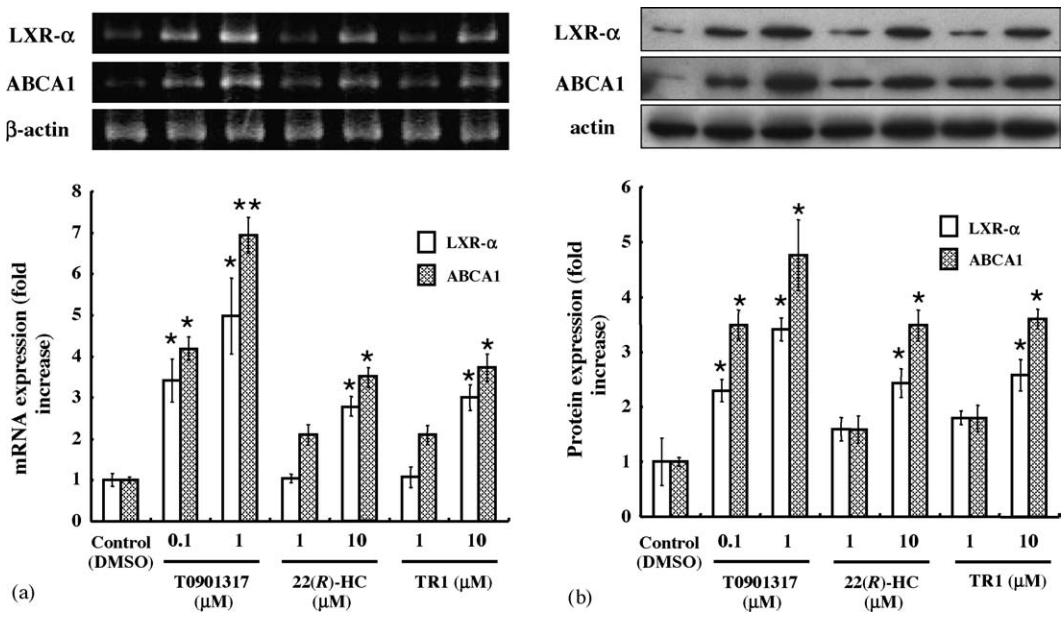

Fig. 3. Effect of TR1 on: (a) LXR-α and ABCA1 mRNA and (b) protein levels in THP-1-derived macrophages. THP-1 monocytes were incubated with PMA (50 ng/mL) for 3 days to differentiate them into adherent macrophages. The macrophages were then treated in the presence and absence of T0901317 (0.1 and 1 μM), 22(*R*)-HC (1 and 10 μM) and TR1 (1 and 10 μM) for 2 days. Total mRNAs and protein were prepared from the cell pellets using TRIzol and cell lysis, respectively. (a) The relative levels of LXR-α and ABCA1 mRNAs were assessed by RT-PCR. Results were normalised to β-actin. Control levels were arbitrarily assigned a value of 1.0. (b) Protein extracts from cells pellets were subjected to SDS-PAGE followed by Western blot analysis using an anti-LXR-α and anti-ABCA1 antibodies. The results are normalised to actin. Control levels were arbitrarily assigned a value of 1.0. All values are means ± S.E.M. ($n = 3$) vs. control, $^{*}p < 0.05$ and $^{**}p < 0.01$.

[47–49]. Differentiation of THP-1 monocyte to macrophage by PMA is typically accompanied by an increased mRNA expression of LXR-α [38,50] and ABCA1 levels [13,39,50]. Agonist activation of LXR also leads to increased protein expression of both LXR-α [34,51,52] and ABCA1 [53,54]. In this study, THP-1 monocytes were rapidly differentiated into adherent macrophages by incubation with PMA (50 ng/mL) for 3 days and then treated with LXR ligands (T0901317 and 22(*R*)-HC) and TR1 for a further 2 days [37,38]. The mRNA and protein were extracted and studied as described in Section 2. The expression of both LXR-α and ABCA1 mRNA levels

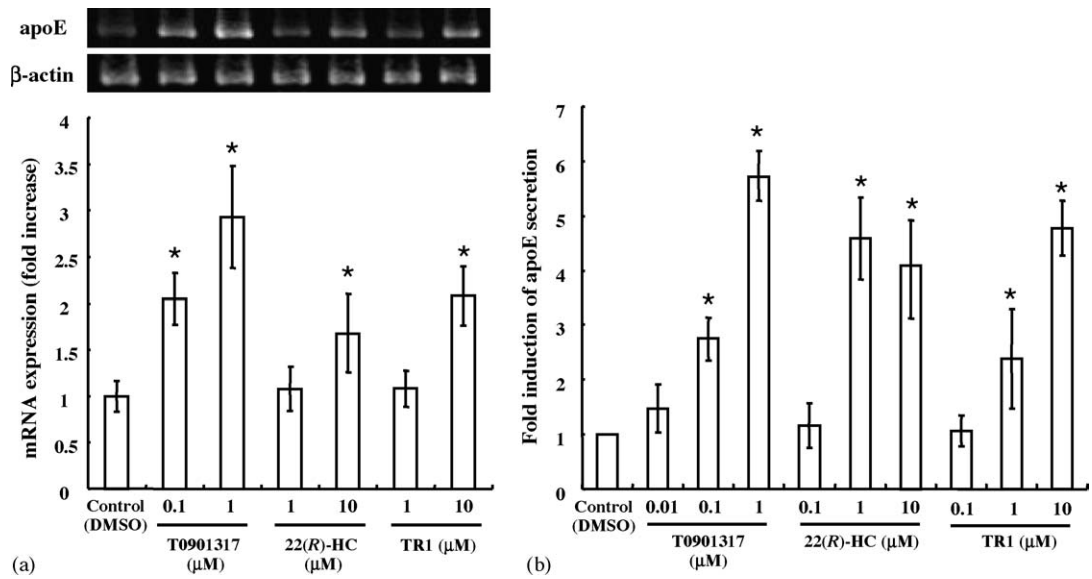

Fig. 4. Effect of TR1 on: (a) apoE mRNA and (b) apoE protein secretion in THP-1-derived macrophages. THP-1 monocytes were incubated with PMA (50 ng/mL) for 3 days to differentiate them into adherent macrophages. The macrophages were then treated for 3 days with 0.77 ng/mL PMA in the presence and absence of T0901317, 22(*R*)-HC and TR1 for a further 2 days. (a) Total mRNAs were prepared from the cell pellets using TRIzol. The relative levels of apoE mRNAs were assessed by RT-PCR. Results were normalised to β-actin. Control levels are arbitrarily assigned a value of 1.0. (b) To determine the level of apoE protein secretion, the supernatants were collected and levels quantified by ELISA. The results were expressed as a fold induction of apoE secretion over vehicle treated control (assigned as 1.0) in the THP-1-derived macrophages. All values are means ± S.E.M. ($n = 3$) vs. control, $^{*}p < 0.05$.

was up-regulated dose-dependently on treatment with T0901317 (positive control), 22(*R*)-HC and TR1, reaching statistical significance relative to control (DMSO only) at 0.1 and 1 μM T0901317 and 10 μM 22(*R*)-HC and TR1 (Fig. 3(a)). This increase in mRNA levels was accompanied by a corresponding increase of LXR-α and ABCA1 protein expression (Fig. 3(b)). The comparable effects of 22(*R*)-HC and TR1 may reflect their structural similarity (Fig. 1). LXR-β expression in the macrophage was not examined in this study because it has been previously shown that LXR-β was not regulated by LXR agonists in either THP-1-derived macrophage or human monocyte-derived macrophages [50] and TR1 showed insignificant up-regulation of LXR-β luciferase activity at the concentrations studied (Fig. 2).

3.4. TR1 induces apoE mRNA expression and secretion in THP-1-derived macrophages

ApoE plays an important role in lipid homeostasis and macrophage-derived apoE is critical for preventing the development of atherosclerotic lesions [24]. To study the effect of TR1 on apoE gene expression and secretion, THP-1 monocytes were differentiated into macrophages by PMA, as described above, prior to treatment with LXR agonists (T0901317 and 22(*R*)-HC) and TR1. The apoE mRNA was assessed by RT-PCR and the amount of apoE protein secreted was determined from the culture medium by an ELISA method. The positive control T0901317 (0.1 and 1 μM) effectively induced apoE mRNA expression and apoE secretion, with a maximum approximately three- and six-fold increase over control, respectively (Fig. 4(a and b)), consistent with previous studies [37,38]. The oxysterol, 22(*R*)-HC increased apoE mRNA by approximately two-fold at 10 μM (Fig. 4(a)) and enhanced apoE secretion optimally at 1 μM (∼4.5-fold) (Fig. 4(b)). TR1 increased apoE mRNA expression and apoE secretion to a similar maximum extent (∼2- and 5-fold, respectively), but required higher concentrations (10 μM) for its optimal effect (Fig. 4(a and b)).

3.5. TR1 docks into the LXR-α and not LXR-β receptor domain

The TR1 ligand occupies a proportionally large volume of the cavity space within the ligand-binding pocket of LXR-α. With an accessible volume of ∼800 Å^3, the ligand-binding pocket can accommodate TR1 (molecular volume of ∼602 Å^3) in a tightly bound conformation restricting it to only a few possible docked poses. TR1

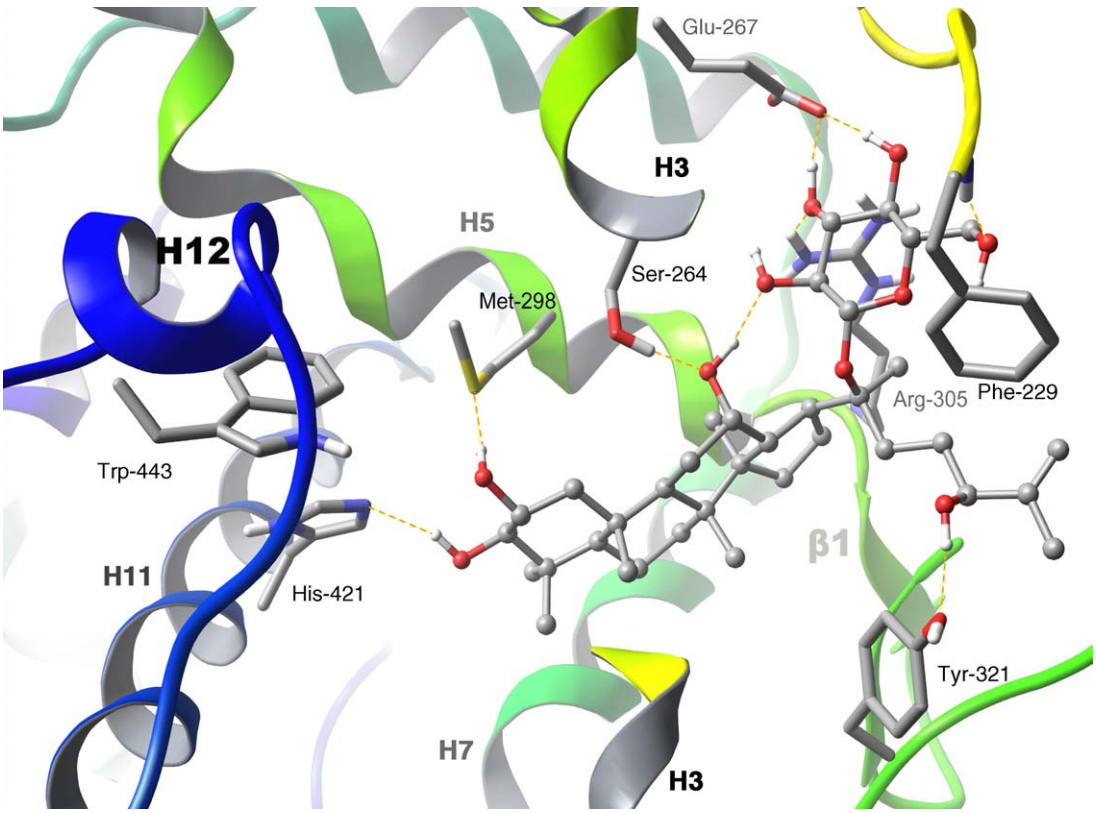

Fig. 5. Proposed complex of TR1 with the ligand-binding pocket of LXR-α. The docked complex was optimised using the OPLS–AA force field in an attempt to reveal flexible side-chain residues that may potentially interact with TR1. The final result suggests the predominant interactions arise from the numerous hydrogen bond contacts (dashed lines) established to the LXR-α receptor. Molecule TR1 and amino acid residues are displayed as ball-and-stick and tube models, respectively. LXR-α is represented in cartoon style, colour coordinated by chain. Residues Glu-259 to Val-263 on Helix 3 (H3) were removed to enhance viewing. Image was created with Maestrov v7.0.

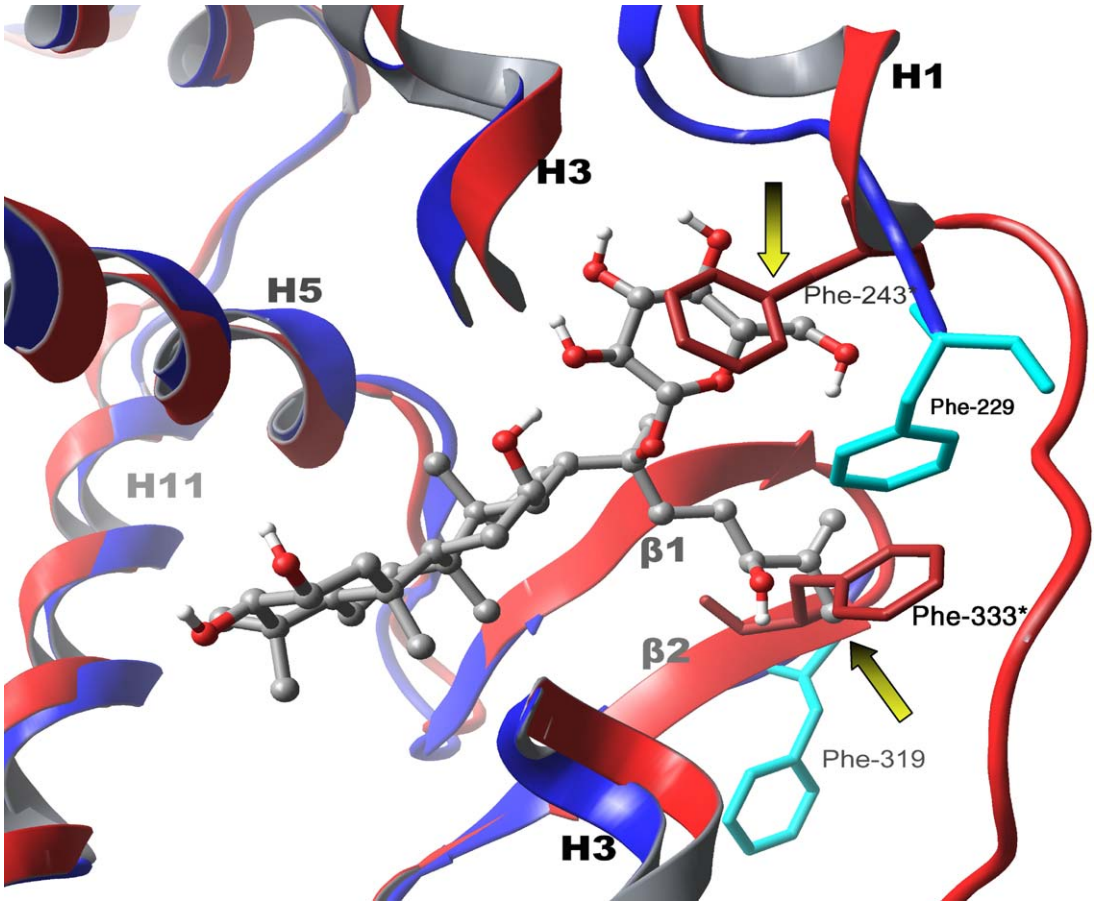

Fig. 6. Superposition of TR1 in the ligand-binding pocket of LXR-α (blue) and LXR-β (red). The superimposed structure of the docked LXR-alpha:TR1 complex with LXR-beta, performed using Swiss-PDB Viewer [64], revealed a small difference in residue orientations. It is speculated TR1 is unable to dock into LXR-β due to steric hindrance from residues Phe-243* and Phe-333* (red), illustrated by the yellow arrows (residues Glu-259/273* to Val-263/Ile-277* on H3 were removed to enhance viewing); (*) indicates residues from LXR-β.

is primarily bound to LXR-α through hydrogen bonding via the many hydroxyl groups present on the molecule (see Fig. 5). Several contacts are established, including those to Met-298, Ser-264, Tyr-321 and to the backbone amide of Phe-229, all within a distances of 2.5 Å. The formation of a hydrogen bond to the Nε imidazole nitrogen of His-421 from the C-3-OH is also evident and appears to be the common contact established by all four ligands. The close proximity of His-421 to Trp-443 (<4 Å) also suggests the potential for these two residues to interact through π–π interactions. TR1-binding involves a network of hydrogen bonds, mediated by the 3′- and 4′-OH groups present on the glucose moiety, bridging residues Glu-267 and Arg-305. An intra-molecular hydrogen bond also forms between the C-12-OH on the C-ring and the oxygen atom from the 2′-OH on the sugar group (Fig. 5).

Conversely, TR1 does not successfully dock into the LXR-β receptor domain. A superposition of the LXR-α:TR1 complex with LXRβ reveals a steric clash between the sugar moiety with Phe-243 and Phe-333 of LXR-β. It appears that this hindrance is not observed in LXR-α as its equivalent phenylalanines, Phe-229 and Phe-319, respectively, adopt different orientations (Fig. 6).

The binding modes of T091317, 22(*R*)-HC and 24(*S*)-HC in LXR-α and LXR-β closely resemble those proposed from previous docking studies [15,16], giving confidence in our model and approach. On the other hand, TR1 did not adopt the same binding orientation as demonstrated by other steroid agonists [15,16]. In such studies, the respective C-22, C-24, C-25 or C-27-OH/epoxide moieties bind to His-421, whilst the C-3-OH group on the A-ring steroidal skeleton is positioned towards the β-strand residues, such as Arg-305 in LXR-α (Arg-319 in LXR-β). In this study, docking results suggest it is the C-3-OH of TR1, which interacts with His-421. Equally, the C-24-OH is placed near Tyr-321, whilst the C-3′ and 4′-OHs from TR1's sugar group makes contact with Arg-305. Hence, the ligand docking study has provided insight into the binding affinity of TR1 to LXR-α receptor.

4. Discussion

Plant medicines have become increasingly popular for the prevention and/or treatment of CVD and have proven to be an abundant source of pharmacological agents for

medicinal purposes [28,29]. Plant extracts have been extensively studied, however, single compounds can ideally provide further information on the mechanism(s) of action of the plant. Coupled with molecular modeling studies, the LBD of the receptor and the agonist can be thus evaluated. This study not only reports on the identification of a new compound, gynosaponin TR1 (Figs. 1 and 2) isolated from *G. pentaphyllum*, but also its selective activation of LXR-α and proposes a receptor–agonist-binding model. Its selectivity in activation of LXR-α over LXR-β may be advantageous, as LXR-α appears to play a dominant role in the liver compared with LXR-β, suggesting that this selectivity of TR1 toward LXR-α may prevent elevation of triglycerides [47,55,56]. However, the dominant role of LXR-α versus LXR-β has only been demonstrated in mice and a recent study has indicated that both isoforms are important for inducing cholesterol efflux [57]. Additionally, human LXR-α, but not LXR-β, is autoregulated, suggesting that the α-isoform is more physiologically responsive to cholesterol loading in humans [13,58]. Thus, the debate of whether selective LXR activators for either LXR-α or LXR-β isoforms or both are more beneficial for preventing or treating atherosclerosis still remains unanswered [12]. Nevertheless, activation of LXR-α has been shown to inhibit the development of atherosclerosis in mice [27] and decrease inflammation by down-regulating genes coding for inducible nitric oxide synthase, cyclooxygenase-2 and interleukin-6, matrix metalloproteinase-9 and tissue factor [59–61].

The current study also showed that TR1 may favourably influence LXR-related pathways. At the same doses, TR1 exhibits comparable efficacy to the natural ligand, 22(*R*)-HC, in THP-1-derived macrophage. This is shown by the induction of expression of a LXR regulated gene, ABCA1, determined by RT-PCR and immunoblotting analysis (Fig. 3). This implies that the induction of ABCA1 by TR1 may promote cholesterol efflux, resulting in a net lipid loss from the macrophage and inhibition of fatty streak formation [9]. Similarly, TR1 was demonstrated to effectively induce apoE, similar to 22(*R*)-HC (Fig. 4). This supports the possibility that TR1 may modulate the RCT pathway via VLDL and chylomicron clearance in macrophages and consequently, decrease susceptibility to atherosclerosis [13,22]. Interestingly, our preliminary study indicated that TR1 weakly activated the lipogenic gene targets sterol-response element-binding protein-1c expression and fatty acid synthase (results not shown), suggesting that TR1 may have different mechanism of action to that of conventional LXR-α agonists, which induce raised TG levels in liver [62,63]. This effect of TR1 in vivo is still under investigation.

Theoretical investigations were employed in an attempt to understand TR1's in vitro activation of the LXR-α receptor over LXR-β. It has been demonstrated in previous studies that the ligand-binding pocket of the LXR isoforms can adopt various shapes and volumes to accommodate a diverse array of ligands with varying size and structure [16,17,19]. This adaptability has encouraged the search for novel LXR agonists. In this study, it was shown that TR1 can dock into LXR-α despite having a larger molecular volume and structure than other more commonly known agonists, such as T0901317. The molecular modeling uncovered possible binding interactions and provided initial clues to TR1's greater selectivity for LXR-α over LXR-β. Together with the current understanding of LXR-α′s ability to interact with various shaped ligands [12,16,17,19], our molecular docking results are consistent with the binding of TR1 to LXR-α and subsequently inducing the in vitro gene expression observed in this study (Figs. 2 and 3).

In previous studies, the interaction of the hydroxyl/epoxide moieties of LXR ligand with His-421 (for LXR-α) and His-435 (for LXR-β) is considered to be the most essential point of contact for LXR:agonist complexes [15–17,19]. A more detailed investigation of the edge-on π-interaction between His-421 (for LXR-α) and His-435 (for LXR-β) mentioned earlier with the neighbouring Trp-443 (for LXR-α) and Trp-457 (for LXR-β), respectively, outlines the crucial determinant for LXR agonistic activity [15–17,19]. In the structures of the LXR-α bound complexes described here, the importance of this relationship is highlighted by the interaction of TR1 through a hydrogen bond made to the Nε of His-421 established from its C-3-OH (distance of 2.0 Å). In addition, the close proximity of His-421 with Trp-443 (distance of 3.7 Å) supports its capability to potentiate agonistic activity towards LXR-α. Other contacts made by TR1, for example to Met-298 and Ser-264 are believed to be involved in either ligand recognition or non-essential interactions of hydroxyl groups to the binding site via hydrogen bonds (Fig. 5).

LXR ligands T0901317, 22(*R*)-HC and 24(*S*)-HC had been previously studied in molecular modeling and were thus assigned as controls in the docking studies [15]. All these agonists appeared to have bound in a similar pose to that published in crystal complexes and docking studies [15–17,19]. In contrast, the results of the docking study of TR1 showed that it bound in a 'reverse' fashion in the LXR-α ligand-binding domain, with the A-ring C-3-OH (Fig. 1) forming the bond to His-421, but not the C-24-OH group, as seen with other sterol agonists. This suggests that the sugar moiety may be a determinant factor for TR1's orientation in the ligand-binding domain. As mentioned, this sugar moiety is not present in the other sterol agonists. Thus, the sugar groups of gypenosides may influence the ligand–receptor interaction. In the case of LXR-β, docking results suggests that TR1 does not fit into the ligand-binding pocket due to steric hindrance from Phe-243 and Phe-333. Unlike their corresponding residues in LXR-α, these phenylalanines in LXR-β project into the ligand-binding pocket, thus prohibiting binding of any molecule larger than the hydroxycholesterols. It is speculated that

this steric hindrance may explain TR1's failure to elicit biological activity in LXR-β (Fig. 6).

In conclusion, we have isolated a novel gynosaponin which functions as an activator-specific for LXR-α from *G. pentaphyllum*. This gynosaponin TR1 has similar activation capacities to that of the hydroxycholesterols and exhibited favourable gene regulatory properties for an LXR modulator. This study provides the first proposed structure–activity relationship of gypenosides on LXR–ligand-binding. Volume and shape of the binding pocket and corresponding gynosaponin ligand, differences in key amino acids involved in the gynosaponin-receptor interaction and the position and stereochemistry of the functional groups of the gynosaponin ligand are important requirements for activation of the LXR receptors. Ultimately, in vivo studies of TR1 would need to be carried out to confirm the in vitro observation and the proposed consequences of these interactions to lipid metabolism and outcome. This study may assist with the development of LXR ligands with beneficial anti-atherogenic properties, without the potential proatherogenic lipogenic effects common to this class of drugs.

Acknowledgements

The authors wish to thank Dr. Yuhao Li, Dr. George Qian Li, Mr. Bruce N. Tattam, Dr. David E. Hibbs and Dr. Maria Tsoli from the University of Sydney and Prof. Gary D. Willet and Dr. James Hook from the University of New South Wales, for their involvement in the project.

References

[1] Libby P. Inflammation in atherosclerosis. Nature 2002;420:868–8674.
[2] Aikawa M, Libby P. Atherosclerotic plaque inflammation: the final frontier? Can J Cardiol 2004;20:631–4.
[3] Stehbens WE. Anitschkow and the cholesterol over-fed rabbit. Cardiovasc Pathol 1999;8:177–8.
[4] Sugiyama S, Okada Y, Sukhova GK, Virmani R, Heinecke JW, Libby P. Macrophage myeloperoxidase regulation by granulocyte macrophage colony-stimulating factor in human atherosclerosis and implications in acute coronary syndromes. Am J Cardiovasc Pathol 2001; 158:879–91.
[5] Jaye M. LXR agonists for the treatment of atherosclerosis. Curr Opin Investig Drugs 2003;4:1053–8.
[6] Repa JJ, Mangelsdorf DJ. The liver X receptor gene team: potential new players in atherosclerosis. Nat Med 2002;8:1243–8.
[7] Tontonoz P, Mangelsdorf DJ. Liver X receptor signaling pathways in cardiovascular disease. Mol Endocrinol 2003;17:985–93.
[8] Kino T, Chrousos GP. Combating atherosclerosis with LXR{alpha} and PPAR{alpha} agonists: is rational multitargeted polypharmacy the future of therapeutics in complex diseases? Mol Interv 2004;4:254–7.
[9] Joseph SB, Tontonoz P. LXRs: new therapeutic targets in atherosclerosis? Curr Opin Pharmacol 2003;3:192–7.
[10] Janowski BA, Grogan MJ, Jones SA, Wisely GB, Kliewer SA, Corey EJ, et al. Structural requirements of ligands for the oxysterol liver X receptors LXRalpha and LXRbeta. Proc Natl Acad Sci USA 1999; 96:266–71.
[11] Ide T, Shimano H, Yoshikawa T, Yahagi N, Amemiya-Kudo M, Matsuzaka T, et al. Cross-talk between peroxisome proliferator-activated receptor (PPAR) alpha and liver X receptor (LXR) in nutritional regulation of fatty acid metabolism. Part II: LXRs suppress lipid degradation gene promoters throughinhibition of PPAR signalling. Mol Endocrinol 2003;17:1255–67.
[12] Collins JL. Therapeutic opportunities for liver X receptor modulators. Curr Opin Drug Discov Dev 2004;7:692–702.
[13] Laffitte BA, Repa JJ, Joseph SB, Wilpitz DC, Kast HR, Mangelsdorf DJ, et al. LXRs control lipid-inducible expression of the apolipoprotein E gene in macrophages and adipocytes. Proc Natl Acad Sci USA 2001;98:507–12.
[14] Sparrow CP, Baffic J, Lam MH, Lund EG, Adams AD, Fu X, et al. A potent synthetic LXR agonist is more effective than cholesterol loading at inducing ABCA1 mRNA and stimulating cholesterol efflux. J Biol Chem 2002;277:10021–7.
[15] Svensson S, Ostberg T, Jacobsson M, Norstrom C, Stefansson K, Hallen D, et al. Crystal structure of the heterodimeric complex of LXRalpha and RXRbeta ligand-binding domains in a fully agonistic conformation. EMBO J 2003;22:4625–33.
[16] Williams S, Bledsoe RK, Collins JL, Boggs S, Lambert MH, Miller AB, et al. X-ray crystal structure of the liver X receptor beta ligand binding domain: regulation by a histidine-tryptophan switch. J Biol Chem 2003;278:27138–43.
[17] Hoerer S, Schmid A, Heckel A, Budzinski RM, Nar H. Crystal structure of the human liver X receptor beta ligand-binding domain in complex with a synthetic agonist. J Mol Biol 2003;334:853–61.
[18] Wang M, Thomas J, Burris TP, Schkeryantz J, Michael LF. Molecular determinants of LXRalpha agonism. J Mol Graph Model 2003; 22:173–81.
[19] Farnegardh M, Bonn T, Sun S, Ljunggren J, Ahola H, Wilhelmsson A, et al. The three-dimensional structure of the liver X receptor beta reveals a flexible ligand-binding pocket that can accommodate fundamentally different ligands. J Biol Chem 2003;278:38821–8.
[20] Mohan R, Heyman RA. Orphan nuclear receptor modulators. Curr Top Med Chem 2003;3:1637–47.
[21] Brooks-Wilson A, Marcil M, Clee SM, Zhang LH, Roomp K, van Dam M, et al. Mutations in ABC1 in Tangier disease and familial high-density lipoprotein deficiency. Nat Genet 1999;22:336–45.
[22] Stefkova J, Poledne R, Hubacek JA. ATP-binding cassette (ABC) transporters in human metabolism and diseases. Physiol Res 2004; 53:235–43.
[23] Orso E, Broccardo C, Kaminski WE, Bottcher A, Liebisch G, Drobnik W, et al. Transport of lipids from golgi to plasma membrane is defective in tangier disease patients and Abc1-deficient mice. Nat Genet 2000;24:192–6.
[24] Bocksch L, Stephens T, Lucas A, Singh B. Apolipoprotein E: possible therapeutic target for atherosclerosis. Curr Drug Targets Cardiovasc Haematol Disord 2001;1:93–106.
[25] Bellosta S, Mahley RW, Sanan DA, Murata J, Newland DL, Taylor JM, et al. Macrophage-specific expression of human apolipoprotein E reduces atherosclerosis in hypercholesterolemic apolipoprotein E-null mice. J Clin Invest 1995;96:2170–9.
[26] Linton MF, Atkinson JB, Fazio S. Prevention of atherosclerosis in apolipoprotein E-deficient mice by bone marrow transplantation. Science 1995;267:1034–7.
[27] Lund EG, Menke JG, Sparrow CP. Liver X receptor agonists as potential therapeutic agents for dyslipidemia and atherosclerosis. Arterioscler Thromb Vasc Biol 2003;23:1169–77.
[28] Huang TH, Kota BP, Razmovski V, Roufogalis BD. Herbal or natural medicines as modulators of peroxisome proliferator activated receptors and related nuclear receptors for therapy of metabolic syndrome. Basic Clin Pharmacol Toxicol 2005;96:3–14.
[29] Bramlett KS, Houck KA, Borchert KM, Dowless MS, Kulanthaivel P, Zhang Y, et al. A natural product ligand of the oxysterol receptor, liver X receptor. J Pharmacol Exp Ther 2003;307:291–6.

[30] Blumert M, Liu JL. Jiaogulan China's "immortality" herb. Badger, USA: Torchlight Publishing Inc., 1999.
[31] Li L, Jiao L, Lau BH. Protective effect of gypenosides against oxidative stress in phagocytes, vascular endothelial cells and liver microsomes. Cancer Biother 1993;8:263–72.
[32] Tanner MA, Bu X, Steimle JA, Myers PR. The direct release of nitric oxide by gypenosides derived from the herb *Gynostemma pentaphyllum*. Nitric Oxide 1999;3:359–65.
[33] Jian Su, New Medical College. The dictionary of Chinese medicine (Zhong Yao Da Ci Dian). Shanghai, China: Shanghai Science and Technology Press; 1986.
[34] Attawish A, Chivapat S, Phadungpat S, Bansiddhi J, Techadamrongsin Y, Mitrijit O, et al. Chronic toxicity of *Gynostemma pentaphyllum*. Fitoterapia 2004;75:539–51.
[35] la Cour B, Molgaard P, Yi Z. Traditional Chinese medicine in treatment of hyperlipidaemia. J Ethnopharmacol 1995;46:125–9.
[36] Yoshikawa K, Takemoto T, Arihara S. Studies on the constituents of Cucurbitaceae plants. Part XVI: on the saponin constituents of *Gynostemma pentaphyllum* Makino (II). Yakugaku Zasshi 1987; 107:262–7.
[37] Perez A, Thuillard JL, Bentzen CL, Niesor EJ. Expression of nuclear receptors and apoE secretion during the differentiation of monocytic THP-1 cells into macrophages. Cell Biol Toxicol 2003;19:95–105.
[38] Quinet EM, Savio DA, Halpern AR, Chen L, Miller CP, Nambi P. Gene-selective modulation by a synthetic oxysterol ligand of the liver X receptor. J Lipid Res 2004;45:1929–42.
[39] Pawar A, Xu J, Jerks E, Mangelsdorf DJ, Jump DB. Fatty acid regulation of liver X receptors (LXR) and peroxisome proliferator-activated receptor alpha (PPARalpha) in HEK293 cells. J Biol Chem 2002;277:39243–50.
[40] Abe A, Kiriyama Y, Hirano M, Miura T, Kamiya H, Harashima H, et al. Troglitazone suppresses cell growth of KU812 cells independently of PPARgamma. Eur J Pharmacol 2002;436:7–13.
[41] Davies GF, McFie PJ, Khandelwal RL, Roesler WJ. Unique ability of troglitazone to up-regulate peroxisome proliferator-activated receptor-gamma expression in hepatocytes. J Pharmacol Exp Ther 2002; 300:72–7.
[42] Wagsater D, Dimberg J, Sirsjo A. Induction of ATP-binding cassette A1 by all-trans retinoic acid: possible role of liver X receptor-α. Int J Mol Med 2003;11:419–23.
[43] Bradford MM. A rapid and sensitive method for the quantitation of microgram quantities of protein utilizing the principle of dye-binding. Anal Biochem 1976;72:248–54.
[44] Mohamadi F, Richard NGJ, Guida WC, Liskamp R, Lipton M, Caufield C, et al. MacroModel—an integrated software system for modeling organic and bioorganic molecules using molecular mechanics. J Comput Chem 1990;11:440.
[45] Friesner RA, Banks JL, Murphy RB, Halgren TA, Klicic JJ, Mainz DT, et al. Glide: a new approach for rapid, accurate docking and scoring. Part 1: method and assessment of docking accuracy. J Med Chem 2004;47:1739–49.
[46] Takemoto T, Arihara S, Yoshikawa K, Kawasaki J, Nakajima T, Okuhira M. Studies on the constituents of Cucurbitaceae plants. Part XI: on the saponin constituents of *Gynostemma pentaphyllum* Makino (7). Yakugaku Zasshi 1984;104:1043–9.
[47] Repa JJ, Turley SD, Lobaccaro JA, Medina J, Li L, Lustig K, et al. Regulation of absorption and ABC1-mediated efflux of cholesterol by RXR heterodimers. Science 2000;289:1524–9.
[48] Schwartz K, Lawn RM, Wade DP. ABC1 gene expression and ApoA-I-mediated cholesterol efflux are regulated by LXR. Biochem Biophys Res Commun 2000;274:794–802.
[49] Venkateswaran A, Laffitte BA, Joseph SB, Mak PA, Wilpitz DC, Edwards PA, et al. Control of cellular cholesterol efflux by the nuclear oxysterol receptor LXR alpha. Proc Natl Acad Sci USA 2000; 97:12097–102.
[50] Whitney KD, Watson MA, Goodwin B, Galardi CM, Maglich JM, Wilson JG, et al. Liver X receptor (LXR) regulation of the LXRalpha gene in human macrophages. J Biol Chem 2001;276:43509–15.
[51] Watanabe Y, Tanaka T, Uchiyama Y, Takeno T, Izumi A, Yamashita H, et al. Establishment of a monoclonal antibody for human LXRalpha: detection of LXRalpha protein expression in human macrophages. Nucl Recept 2003;1:1–6.
[52] Kaneko E, Matsuda M, Yamada Y, Tachibana Y, Shimomura I, Makishima M. Induction of intestinal ATP-binding cassette transporters by a phytosterol-derived liver X receptor agonist. J Biol Chem 2003;278:36091–8.
[53] Sun Y, Yao J, Kim TW, Tall AR. Expression of liver X receptor target genes decreases cellular amyloid beta peptide secretion. J Biol Chem 2003;278:27688–94.
[54] Wang Y, Kurdi-Haidar B, Oram JF. LXR-mediated activation of macrophage stearoyl-CoA desaturase generates unsaturated fatty acids that destabilize ABCA1. J Lipid Res 2004;45:972–80.
[55] Alberti S, Schuster G, Parini P, Feltkamp D, Diczfalusy U, Rudling M, et al. Hepatic cholesterol metabolism and resistance to dietary cholesterol in LXRbeta-deficient mice. J Clin Invest 2001;107:565–73.
[56] Lala DS. Liver X receptors and atherosclerosis. IDrugs 2004;7:563–9.
[57] Schuster GU, Parini P, Wang L, Alberti S, Steffensen KR, Hansson GK, et al. Accumulation of foam cells in liver X receptor-deficient mice. Circulation 2002;106:1147–53.
[58] Li Y, Bolten C, Bhat BG, Woodring-Dietz J, Li S, Prayaga SK, et al. Induction of human liver X receptor alpha gene expression via an autoregulatory loop mechanism. Mol Endocrinol 2002;16:506–14.
[59] Castrillo A, Joseph SB, Marathe C, Mangelsdorf DJ, Tontonoz P. Liver X receptor-dependent repression of matrix metalloproteinase-9 expression in macrophages. J Biol Chem 2003;278:10443–9.
[60] Joseph SB, Castrillo A, Laffitte BA, Mangelsdorf DJ, Tontonoz P. Reciprocal regulation of inflammation and lipid metabolism by liver X receptors. Nat Med 2003;9:213–9.
[61] Terasaka N, Hiroshima A, Ariga A, Honzumi S, Koieyama T, Inaba T, et al. Liver X receptor agonists inhibit tissue factor expression in macrophages. FEBS J 2005;272:1546–56.
[62] Ginsberg HN. New perspectives on atherogenesis: role of abnormal triglyceride-rich lipoprotein metabolism. Circulation 2002;106:2137–42.
[63] Tontonoz P, Mangelsdorf DJ. Liver X receptor signaling pathways in cardiovascular disease. Mol Endocrinol 2003;17:985–93.
[64] Guex N, Peitsch MC. SWISS-MODEL and the Swiss-PdbViewer: an environment for comparative protein modelling. Electrophoresis 1997;18:2714–23.